Biogeosciences

Supplement of

Effect of straw retention and mineral fertilization on P speciation and P-transformation microorganisms in water-extractable colloids of a Vertisol

Shanshan Bai et al.

Correspondence to: Xiaoqian Jiang (jiangxq7@mail.sysu.edu.cn)

Table S1 Chemical shift of peaks detected in ^{31}P-NMR spectra of NaOH-Na$_2$EDTA samples

Category[a]	P form or compound class	Chemical Shift (ppm)
Inorganic P		
	Orthophosphate	6.0
	Pyrophosphate	-4.39±0.03
Organic P		
Orthophosphate Monoesters		
	myo-IHP	4.28±0.01, 4.44±0.02, 4.81±0.01, 5.71±0.02
	scyllo-IHP	3.96±0.02
	α-glyc	5.01±0.02
	β-glyc	4.66±0.02
Orthophosphate diesters-- DNA		-0.41±0.04

[a]myo-inositol hexakisphosphate (myo-IHP), scyllo-inositol hexakisphosphate (scyllo-IHP), α-glycerophosphate (α-glyc), β-glycerophosphate (β-glyc).

Table S2 The KO number, function descriptions, gene name and classification of the investigated genes referring to KEGG database

| Classification	KO number	Details for gene function	Corresponding gene
Genes involved in inorganic P-solubilization	K00117	quinoprotein glucose dehydrogenase	*gcd*
	K01507	inorganic pyrophosphatase	*ppa*
	K00937	Polyphosphate kinase	*ppk*
	K01524	exopolyphosphatase / guanosine-5'-triphosphate,3'-diphosphate pyrophosphatase	*ppx*
Genes involved in organic P-mineralization	K05774	C-P lyase subunit, ribose 1,5-bisphosphokinase	*phnN*
	K00111	Glycerol-3-phosphate dehydrogenase	*glpA*
	K00112	Glycerol-3-phosphate dehydrogenase subunit B	*glpB*
	K00113	Glycerol-3-phosphate dehydrogenase subunit C	*glpC*
	K00864	Glycerol kinase glpK	*glpK*
	K01083	3-Phytase	*phy*
	K01093	4-phytase	*appA*
	K01126	glycerophosphoryl diester phosphodiesterase	*ugpQ*
	K01077	alkaline phosphatase	*phoA*
	K01113	alkaline phosphatase	*phoD*
	K09474	acid phosphatase (class A)	*phoN*
	K03788	acid phosphatase (class B)	*aphA*
Genes involved in P-starvation response regulation	K07636	two-component system, OmpR family, phosphate regulon sensor histidine kinase PhoR	*phoR*
	K07657	two-component system, OmpR family, phosphate regulon response regulator PhoB	*phoB*
Genes involved in P-uptake and transport system	K05813	Glycerol-3-phosphate transporter subunit, periplasmic-binding component	*ugpB*
	K05814	Glycerol-3-phosphate transporter subunit	*ugpA*
	K05815	Glycerol-3-phosphate transporter subunit, membrane component	*ugpE*
	K05816	Glycerol-3-phosphate transporter subunit, ATP-binding component	*ugpC*
	K02041	phosphonate transport system, ATP-binding component	*phnC*
	K02042	phosphonate transport system, membrane component	*phnE*
	K02044	phosphonate transport system, periplasmic-binding component	*phnD*
	K02036	phosphate transport system, ATP-binding component	*pstB*
	K02037	phosphate transport system, membrane component	*pstC*
	K02038	phosphate transport system, membrane component	*pstA*
	K02040	phosphate transport system, periplasmic-binding component	*pstS*
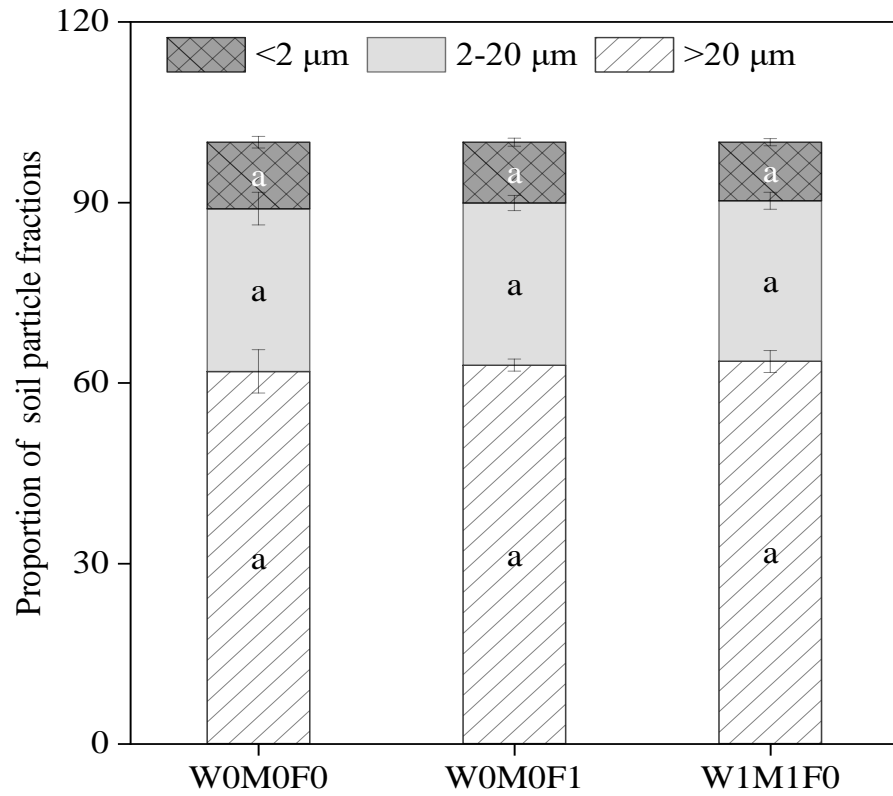
Fig. S1 Proportion of water-dispersible soil particle fractions for the W0M0F0, W0M0F1 and W1M1F0 treatments
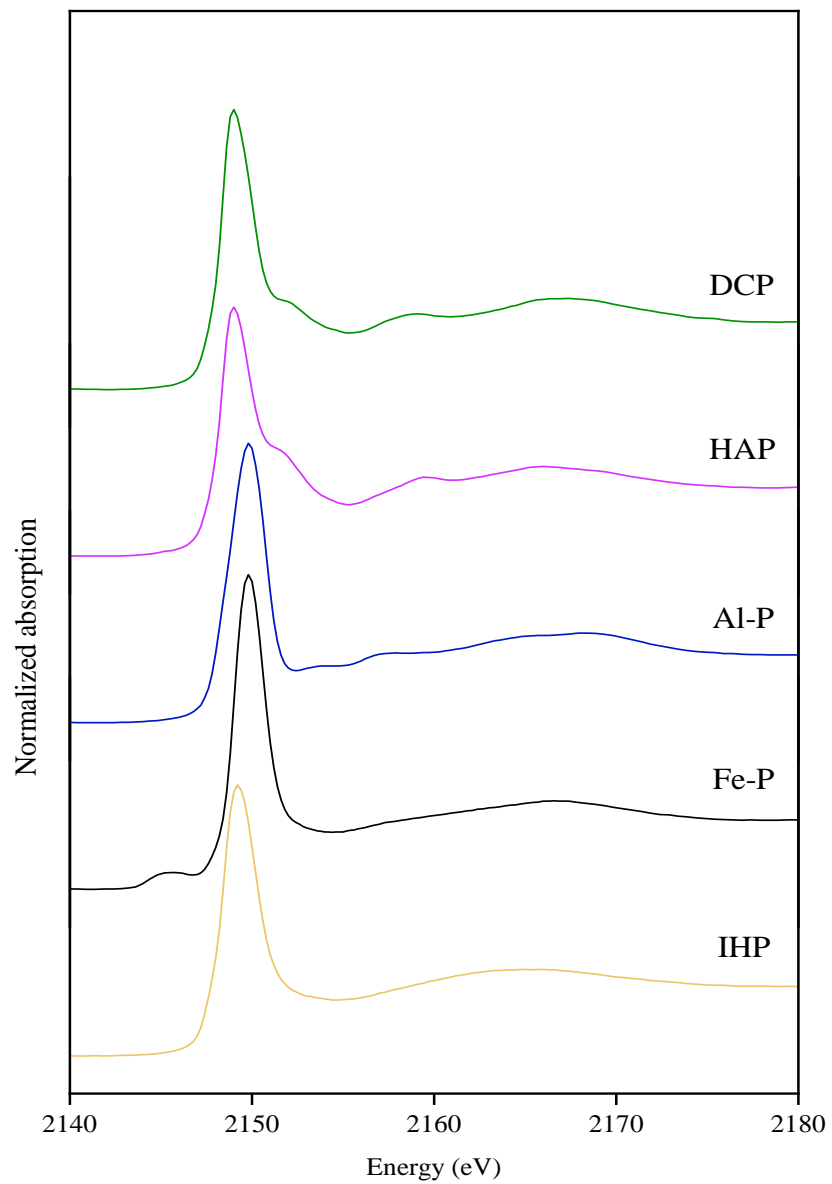
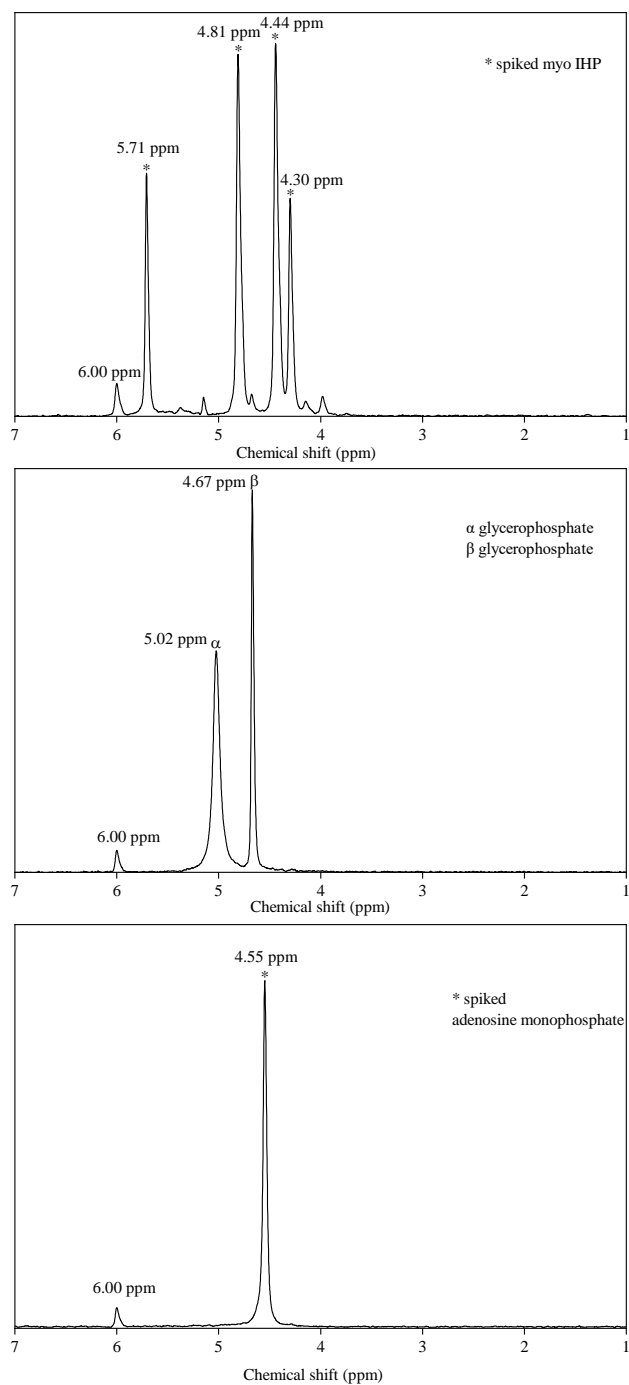Figure S2 Phosphorus K-edge XANES spectra of P reference compounds

Fig. S3 The solution ^{31}P NMR spectrum of a NaOH-Na$_2$EDTA extract of the W0M0F0 bulk soil spiked with a) myo-inositol hexakisphosphate (Myo−IHP), b) α- glycerophosphate and β- glycerophosphate, and c) adenosine monophosphate.
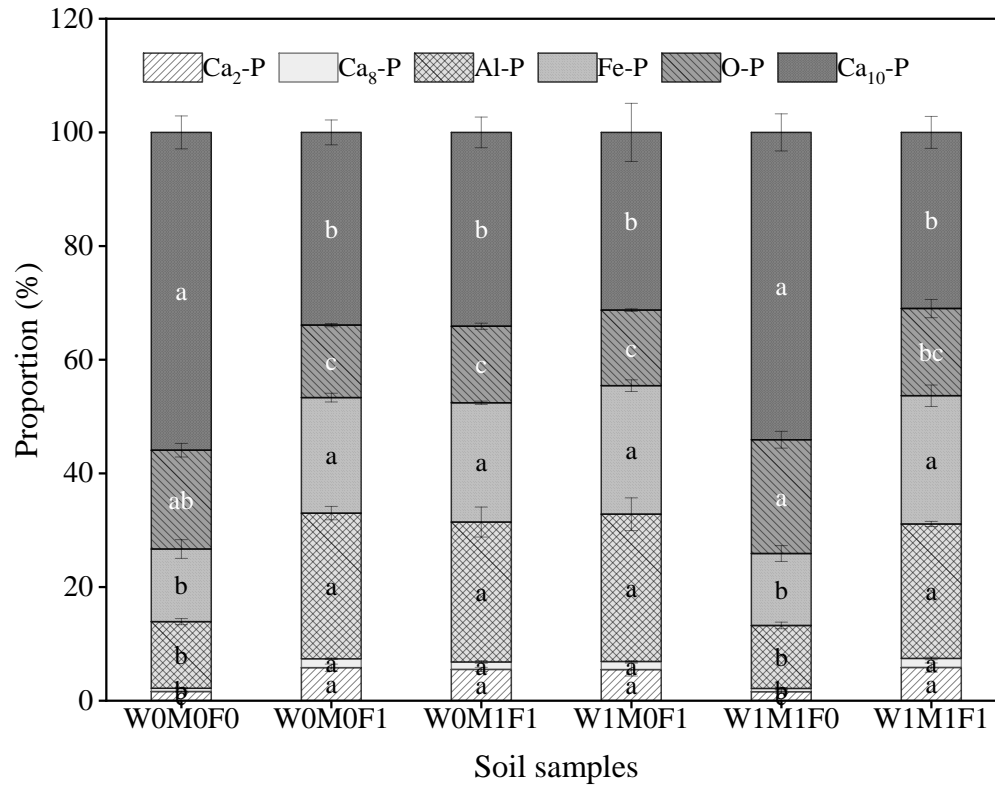
Fig. S4 Proportion of different soil inorganic phosphorus fractions in bulk soil
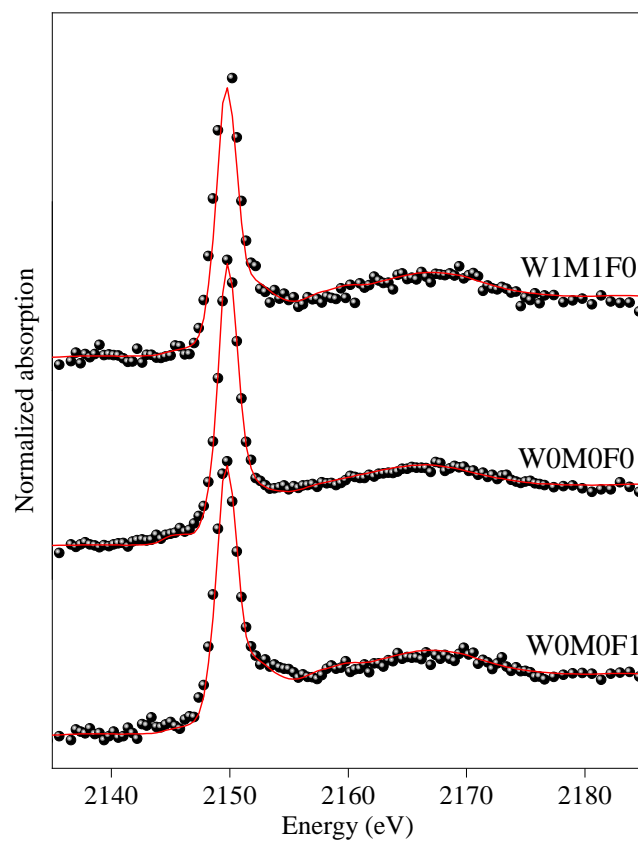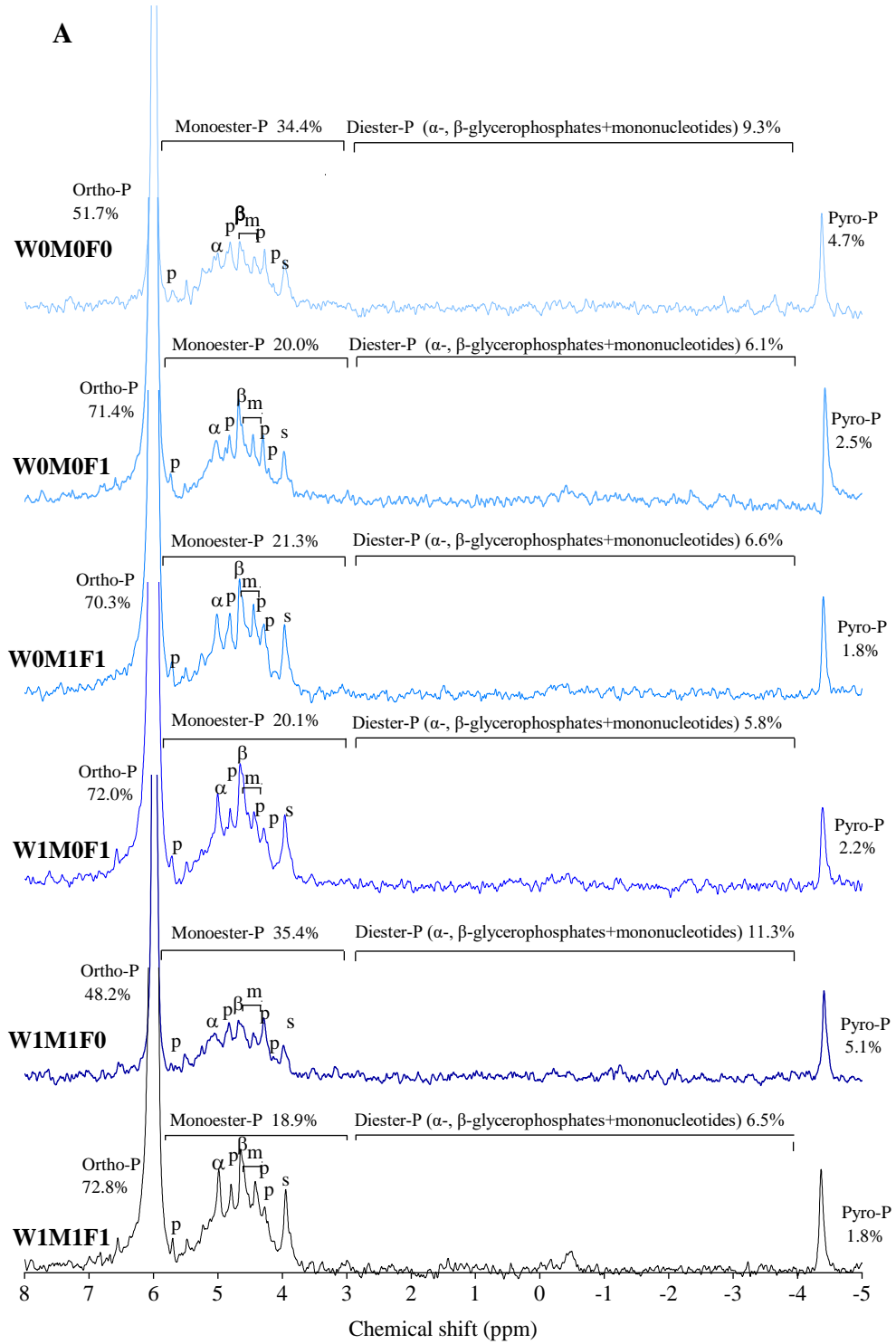
Fig. S5 Results of the linear combination fitting (LCF) of the P K- edge XANES spectra for water-extractable colloids (WECs) of the W0M0F0, W0M0F1 and W1M1F0 treatments. The raw data is represented by points and the fitting results are shown by solid lines.
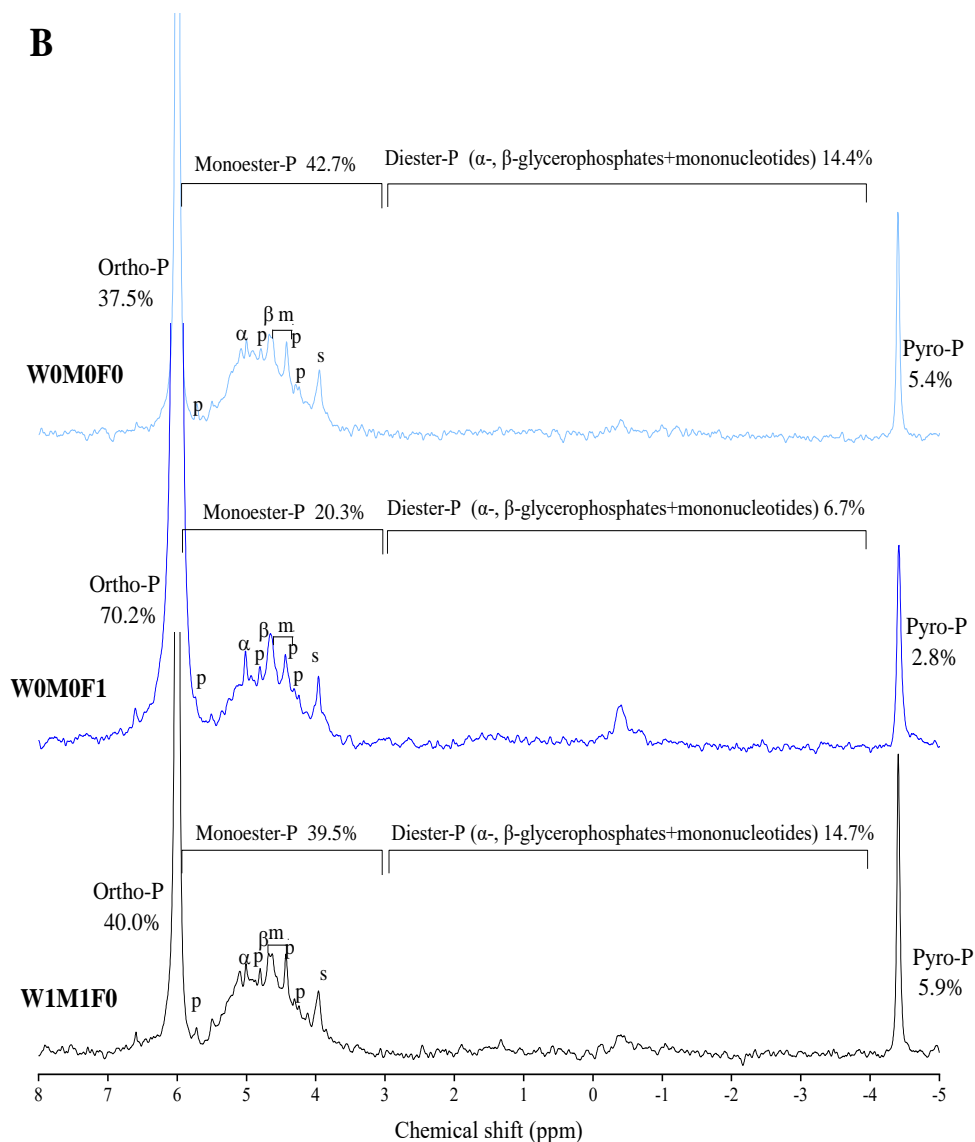
A

W0M0F0 — Ortho-P 51.7%; Monoester-P 34.4%; Diester-P (α-, β-glycerophosphates+mononucleotides) 9.3%; Pyro-P 4.7%

W0M0F1 — Ortho-P 71.4%; Monoester-P 20.0%; Diester-P (α-, β-glycerophosphates+mononucleotides) 6.1%; Pyro-P 2.5%

W0M1F1 — Ortho-P 70.3%; Monoester-P 21.3%; Diester-P (α-, β-glycerophosphates+mononucleotides) 6.6%; Pyro-P 1.8%

W1M0F1 — Ortho-P 72.0%; Monoester-P 20.1%; Diester-P (α-, β-glycerophosphates+mononucleotides) 5.8%; Pyro-P 2.2%

W1M1F0 — Ortho-P 48.2%; Monoester-P 35.4%; Diester-P (α-, β-glycerophosphates+mononucleotides) 11.3%; Pyro-P 5.1%

W1M1F1 — Ortho-P 72.8%; Monoester-P 18.9%; Diester-P (α-, β-glycerophosphates+mononucleotides) 6.5%; Pyro-P 1.8%

Chemical shift (ppm)

Fig. S6 Solution ^{31}P NMR spectra of NaOH–Na$_2$EDTA extracts of bulk soil (A) and water-extractable colloids (WECs, B)

The signals were assigned as follows: orthophosphate (Ortho-P); orthophosphate monoester (Monoester-P); orthophosphate diesters (Diesters-P); pyrophosphate (Pyro-P); myo-inositol hexakisphosphate (p); syllo-inositol hexakisphosphate (s); mononucleotides (m); α-glycerophosphate (α); β-glycerophosphate (β). Calculation by including diester degradation products (i.e., Glyc+nucl: α/β- glycerophosphate and mononucleotides) with Diesters-P rather than Monoesters-P. The percentage indicated the proportion of each phosphorus compounds fraction to the extracted-P.
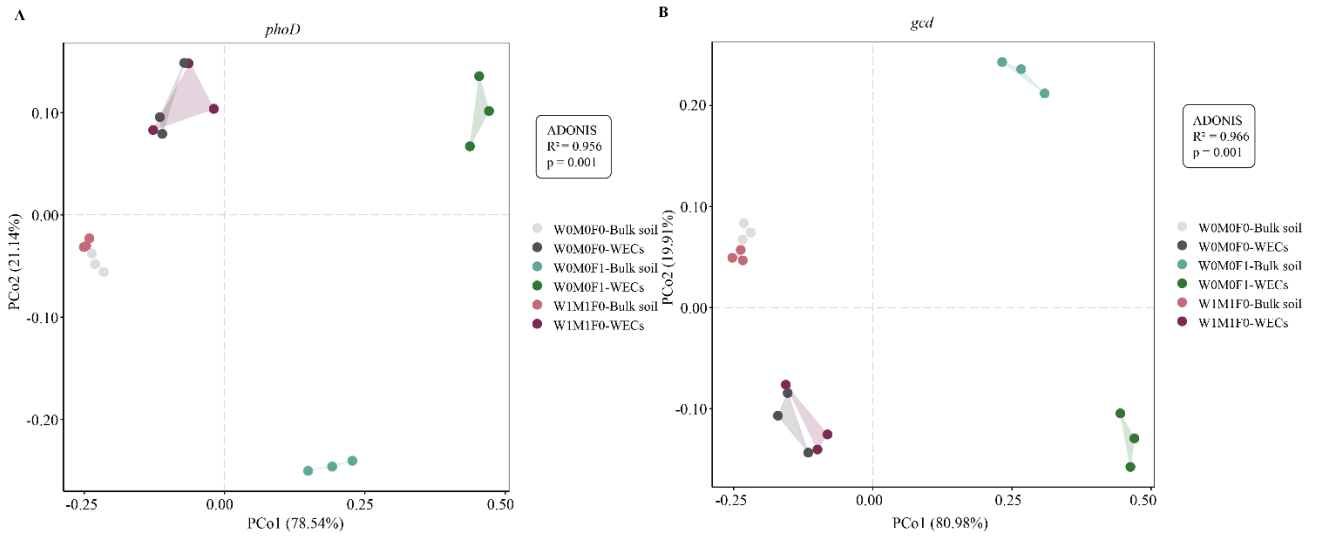
Fig. S7 Principal coordinate analysis (PCoA) of microbial community for *phoD* (A) and *gcd* (B)gene in bulk soils and water-extractable colloids (WECs)
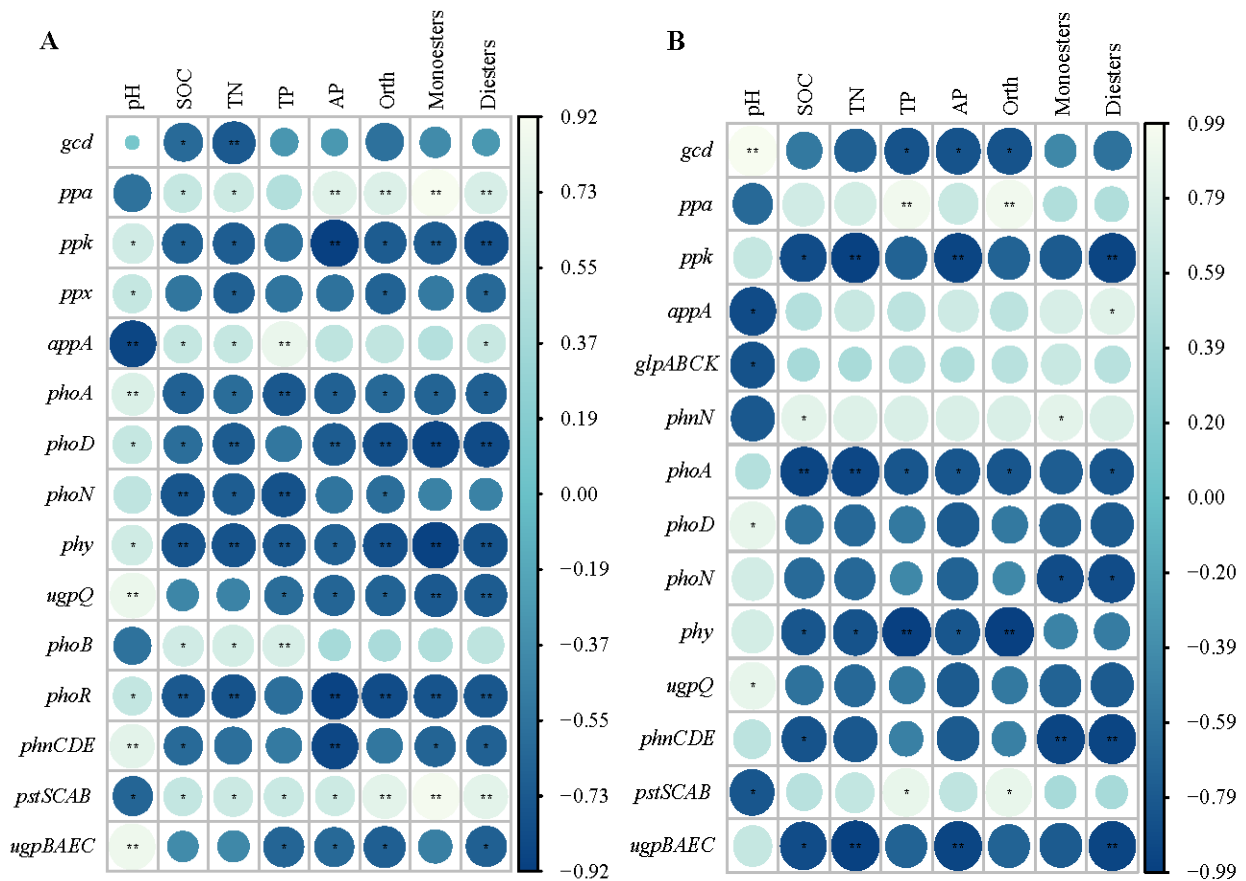
Fig. S8 Spearman correlation heatmap of P-cycling genes and soil nutrients in bulk soils (A) and water-extractable colloids (WECs, B)

The relative abundance of *phn* transporter systems was calculated as the average abundances of gene *phnC*, *phnD*, and *phnE*; the *pst* transporter systems was calculated as the average abundances of gene *pstS*, *pstC*, *pstA*, and *pstB*; The *ugp* transporter systems was calculated as the average abundances of gene *ugpB*, *ugpA*, *ugpE*, and *ugpC*. Soil properties include soil pH, soil organic carbon (SOC), total nitrogen (TN), total phosphorus (TP), available P (AP), orthophosphate (Orth), orthophosphate monoesters (Monoesters), orthophosphate diesters (Diesters). Asterisks indicate a significant association between the abundance of a given functional gene and particular soil properties: **, *p* <0.01; *, *p* <0.05.